Simple Analytic Formulas for the Nonlocal Field Generated by Circuit Elements in Multilayer Structures

Robert W. Jackson, *Senior Member, IEEE*

***Abstract*—Simple analytic expressions are derived for the distant field generated by surface currents or via currents in a three-dielectric-layer parallel-plate structure. These expressions are useful for coupling calculations applied to microwave multichip assemblies. Their simplicity results from making low-frequency approximations; however, their accuracy is sufficient for coupling calculations up to millimeter-wave frequencies in typical structures. They are validated by comparison to numerically determined results. Examination of these equations reveals some general characteristics of coupling in multilayer configurations.**

***Index Terms*—Ball grid arrays, coupling, microwave multichip assemblies, microwave multichip modules, microwave packaging, multilayer structures, mutual impedance, parallel-plate modes.**

I. Introduction

THERE ARE many situations in microwave and millimeter-wave packaging where one is concerned with undesirable coupling between circuit elements. These cases often involve multiple dielectric layers bounded on the top and bottom by conducting planes. Examples include stripline circuits, microstrip circuits with a shield, or modern low-cost packages such as ball grid arrays (BGAs), multilayer ceramic packages, or other multichip modules. Circuits usually consist of surface currents on the interfaces between layers and vias through layers. When circuit elements are close to each other, they couple by means of their reactive fields (capacitive or inductive). When there is more separation, they couple by means of a propagating parallel-plate wave. This paper is concerned with the latter.

Calculating the voltage generated at one point due to a current at another point (the mutual impedance) can be obtained by numerical means [1], [2]. This has been done for many years, and for very complicated structures, it is the best way to proceed. However, for many cases, a simplified analytic expression would be good enough, and would lend some physical insight into the layer characteristics that promote or inhibit coupling.

In this paper, we derive a set of approximate analytic expressions for the electric fields at one point due to surface currents or via currents at another point. We will focus on the case of three dielectric layers between two conducting planes, as illustrated in Fig. 1. We make several key approximations as follows:

1) source and field points are separated enough that no evanescent field coupling occurs;
2) conducting planes are sufficiently close together that only the lowest order parallel-plate mode propagates in the dielectrics;
3) frequencies of interest are low enough that the parallel-plate mode is quasi-TEM.

These requirements are satisfied in many practical structures for frequencies into the millimeter-wave range. The expressions are derived for fields emanating from short current elements on interface surfaces (electric dipoles) and for uniform currents extending through any one of the layers shown in Fig. 1. These current elements could be part of a more complicated element, e.g., a grounded spiral inductor or a transmission line, or they could also be equivalent sources for an entire microwave integrated circuit (IC) in a multichip module [3].

In Section II, the simplified expressions are derived. Section III shows some verification results. Lastly, we discuss the implications of these expressions and draw conclusions.

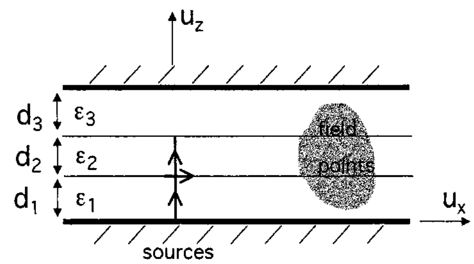

Fig. 1. Three-layer parallel-plate configuration where via and surface currents at $\rho = 0$ generate fields at a distance.

II. Derivation of Simplified Formula

Referring to Fig. 1, we consider a set of via currents or surface currents located at the origin creating fields at some distance ρ where they may couple to other circuit elements. In general, these currents excite fields that can be expressed as a combination of TM to z-fields and TE to z-fields. Exact expressions for these fields can be written in terms of complicated spectral integrals [4]. If the cover and ground planes are sufficiently close together, all the TE fields of the structure are evanescent and, at large ρ, they decay to a negligible level. This leaves only the TM fields. These can be written in terms of a z-directed magnetic potential as follows.

Manuscript received February 3, 2000. This work was supported by the Defense Advanced Research Projects Agency under the MAFET Thrust 1 Program.

The author is with the Department of Electrical and Computer Engineering, University of Massachusetts at Amherst, Amherst, MA 01003 USA.

Publisher Item Identifier S 0018-9480(00)09549-1.

When the source is an x-directed unit dipole at $\rho = 0$, $z = d_1$, the potential at large ρ is

$$A_z(x, y, d_1) = \frac{\partial}{\partial x}\int\int \frac{dk_x dk_y}{(2\pi)^2} e^{jk_x x} e^{jk_y y}\left(\frac{Y_{LM}^{(1)}(\beta)}{\beta^2 Y_M(\beta)}\right) = \frac{\partial}{\partial x}F^{-1}\left(\frac{Y_{LM}^{(1)}(\beta)}{\beta^2 Y_M(\beta)}\right) \quad (1)$$

where $\beta^2 \equiv k_x^2 + k_y^2$, the operator $F^{-1}()$ is defined to be the inverse Fourier transform, and the functions, $Y_{LM}^{(1)}$, Y_M are defined in Appendix A. For a y-directed unit dipole, the derivative in (1) is taken with respect to y rather than x.

For a z-directed filamentary current I, located at $\rho = 0$ and extending from $z = 0$ to $z = d_1$ with a strength such that $Id_1 = 1$

$$A_z(x, y, d_1) = F^{-1}(Z_1(\beta)) \quad (2a)$$

where

$$Z_1(\beta) \equiv -\frac{Y_{\mathrm{RM}}^{(2)}(\beta)}{k_{zi}^2 d_1 Y_M(\beta)} \quad (2b)$$

$k_{zi}^2 \equiv (\varepsilon_{ri}k_0^2 - \beta^2)$, and $Y_{\mathrm{RM}}^{(2)}$ is defined in Appendix A. For a filamentary current located at $\rho = 0$ and extending from $z = d_1$ to $z = d_2$ with a strength such that $Id_2 = 1$

$$A_z(x, y, d_1) = F^{-1}\left(\frac{Y_{LM}^{(1)}\left[Y_{\mathrm{RM}}^{(3)}\sin(k_{z2}d_2) + jY_{\mathrm{TM}}^{(2)}(1-\cos(k_{z2}d_2))\right]}{k_{z2}^2 d_2\left[jY_{\mathrm{TM}}^{(2)}\cos(k_{z2}d_2) - Y_{\mathrm{RM}}^{(3)}\sin(k_{z2}d_2)\right]Y_M}\right) \quad (3)$$

and, as before, the admittance functions is defined in Appendix A.

Equations (1)–(3) are all rigorous expressions for the TM part of the fields generated by the current elements described above. In what follows, we focus on (2). Equations (1) and (3) can be simplified using the same procedure.

The inverse Fourier transform in (2) can be converted into an infinite sum with each term corresponding to a pole of $Z_1(\beta)$ [4]. The pole values of β are solutions of $Y_M(\beta) = 0$ and are the TM parallel plate mode propagation constants. At low frequencies, all such modes are evanescent, except for the lowest order mode, i.e., the TM_0 mode, which propagates for all frequencies. For large ρ, only the TM_0 term in the summation is important as all other terms have decayed to negligible size. Thus, for large ρ, (2a) becomes

$$A_z(x, y, d_1) = \frac{-j\beta_0^{TM}}{2}\mathrm{Res}\left[Z_1\left(\beta_0^{\mathrm{TM}}\right)\right]H_0^{(2)}(\beta_0^{\mathrm{TM}}\rho) \quad (4)$$

where $\mathrm{Res}[Z_1]$ is the residue of Z_1 at the pole $\beta = \beta_0^{\mathrm{TM}}$.

Up to this point, the only approximations that have been used is that all the TE and TM modes excited by the current at $\rho = 0$ have decayed away at large ρ, except for the TM_0 mode. This kind of analysis is not particularly new, and (4) is still very complicated. Next, however, we make more drastic simplifications. We start by taking the expression for Y_M in Appendix A and rewriting it here

$$Y_M = -jY_{\mathrm{TM}}^{(1)}\cot(k_{z1}d_1) + Y_{\mathrm{TM}}^{(2)}\frac{-jY_{TM}^{(3)}\cot(k_{z3}d_3) + jY_{\mathrm{TM}}\tan(k_{z2}d_2)}{Y_{\mathrm{TM}}^{(2)} + Y_{\mathrm{TM}}^{(3)}\cot(k_{z3}d_3)\tan(k_{z2}d_2)}. \quad (5)$$

By assuming $k_{zi}d_i \ll 1$, we get

$$Y_M \approx -j\frac{\varepsilon_{r1}k_o}{\eta_o k_{z1}^2 d_1} + \frac{\varepsilon_{r2}k_o}{\eta_o k_{z2}}\frac{-j\dfrac{\varepsilon_{r3}}{k_{z3}^2 d_3} + j\varepsilon_{r2}d_2}{\dfrac{\varepsilon_{r2}}{k_{z2}} + \dfrac{\varepsilon_{r3}k_{z2}d_2}{k_{z3}^2 d_3}}. \quad (6)$$

Further simplification occurs by assuming $\varepsilon_{r3}/k_{z3}^2 d_3 \gg \varepsilon_{r2}d_2$. We also rewrite k_{zi}^2 as $k_{zi}^2 = k_o^2\varepsilon_{ri} - \beta^2 = k_o^2(\varepsilon_{ri} - \varepsilon_e)$ where $\varepsilon_e \equiv (\beta/k_o)^2$. Equation (6) then becomes

$$Y_M(\beta) = \frac{-j}{\eta_o k_o} \cdot \left[\frac{1}{\frac{d_1}{\varepsilon_{r1}}(\varepsilon_{r1} - \varepsilon_e)} + \frac{1}{\dfrac{d_2}{\varepsilon_{r2}}(\varepsilon_{r2} - \varepsilon_e) + \dfrac{d_3}{\varepsilon_{r3}}(\varepsilon_{r3} - \varepsilon_e)}\right] \quad (7)$$

By setting $Y_M = 0$, we can solve for ε_e, the effective dielectric constant of the TM_o mode. This yields the not surprising result

$$\varepsilon_e = \frac{d_1 + d_2 + d_3}{\dfrac{d_1}{\varepsilon_{r1}} + \dfrac{d_2}{\varepsilon_{r2}} + \dfrac{d_3}{\varepsilon_{r3}}} \quad (8)$$

which is an extension of the two-layer expression found in an exercise in Harrington's textbook [5, Ch. 4, Problem 4–13].

The residue in (4) can be determined by examining Z_1 in (2b) and noting that $\partial Y_M/\partial\beta$ is needed. Taking the derivative of (7) and using (8) results in

$$\left.\frac{\partial Y_M}{\partial\beta}\right|_{\beta=\beta_o^{\mathrm{TM}}} = -j\frac{2\sqrt{\varepsilon_e}}{\eta k_o^2}\frac{\dfrac{d_1}{\varepsilon_{r1}} + \dfrac{d_2}{\varepsilon_{r2}} + \dfrac{d_3}{\varepsilon_{r3}}}{\left(\dfrac{d_1}{\varepsilon_{r1}}\right)^2(\varepsilon_{r1} - \varepsilon_e)^2}. \quad (9)$$

The residue of Z_1 can now be simplified to

$$\mathrm{Res}(Z_1) = \frac{-Y_{\mathrm{RM}}^{(2)}}{k_{z1}^2 d_1}\left[\frac{\partial Y_M}{\partial\beta}\right]_{\beta=\beta_o^{\mathrm{TM}}}^{-1} \approx \frac{-j/(\varepsilon_{r1}\eta k_o^3)}{\left(\dfrac{d_1}{\varepsilon_{r1}}\right)^2(\varepsilon_{r1} - \varepsilon_e)^2}\left[\frac{\partial Y_M}{\partial\beta}\right]_{\beta=\beta_o^{\mathrm{TM}}}^{-1} = \frac{\sqrt{\varepsilon_e}}{2\varepsilon_{r1}k_o(d_1 + d_2 + d_3)} \quad (10)$$

where the same low-frequency approximations were used to simplify $Y_{\mathrm{RM}}^{(2)}$ as were used to simplify (5). This finally reduces (4) to

$$A_z(x, y, d_1) = \frac{-j\varepsilon_e}{4\varepsilon_{r1}(d_1 + d_2 + d_3)}H_o^{(2)}\left(\beta_0^{\mathrm{TM}}\rho\right) \quad (11)$$

which, to repeat, is the potential at large ρ due to a uniform filamentary current located a $\rho = 0$ and extending through layer 1 such that $Id_1 = 1$.

Similar manipulations of (3) results in the potential emitted from a unit uniform filamentary current extending through layer 2 with $Id_2 = 1$

$$A_z(x, y, d_1) = \frac{-j\varepsilon_e}{4\varepsilon_{r2}(d_1 + d_2 + d_3)} H_o^{(2)}\left(\beta_0^{\mathrm{TM}}\rho\right). \quad (12)$$

Likewise, in (1), the potential due to unit x-directed unit electric dipoles on the surface of substrate 1 can be simplified to

$$A_z(x, y, d_1) = \frac{-j(\varepsilon_{r1} - \varepsilon_e)}{4\varepsilon_{r1}(d_1 + d_2 + d_3)} d_1 \frac{\partial}{\partial x} H_o^{(2)}\left(\beta_0^{\mathrm{TM}}\rho\right). \quad (13)$$

(For a y-directed source dipole, the derivative is taken with respect to y rather than x.) Although (11)–(13) only give the potential at $z = d_1$, the potential is due solely to the TM_o parallel-plate mode and, thus, can easily be written for all z in terms of the potential at $z = d_1$ (See Appendix B).

The electric fields at the observation point can be exactly related to the potential A_z by

$$E_z(x, y, z) = \frac{\left(\beta_0^{\mathrm{TM}}\right)^2}{j\omega\varepsilon_o\varepsilon_{ri}} A_z(x, y, z) \quad (14a)$$

$$E_u(x, y, z) = \frac{1}{j\omega\varepsilon_o\varepsilon_{ri}} \frac{\partial^2}{\partial u \partial z} A_z(x, y, z) \quad (14b)$$

where $u = x$ or y depending on the electric-field component desired. The index $i = 1, 2, 3$ depends on the layer in which the observation is being made. The electric-field functions are still somewhat complicated, but if we again make use of the $k_{zi}d_i \ll 1$ the potential, A_z becomes independent of z to the lowest order. If, in addition, we write β_o^{TM} in terms of ε_e, (14a) and (14b) simplify to

$$E_z(x, y, z) = \frac{-jk_o\eta_o\varepsilon_e}{\varepsilon_{ri}} A_z(x, y, d_1) \quad (15a)$$

$$E_u(x, y, d_1) = \frac{jk_o\eta_o(\varepsilon_{r1} - \varepsilon_e)}{\varepsilon_{r1}} d_1 \frac{\partial}{\partial u} A_z(x, y, d_1) \quad (15b)$$

$$E_u\big(x, y, (d_1 + d_2)\big) = \frac{-jk_o\eta_o(\varepsilon_{r3} - \varepsilon_e)}{\varepsilon_{r3}} d_3 \frac{\partial}{\partial u} A_z(x, y, d_1) \quad (15c)$$

where E_z is valid at all z and E_x, E_y are valid only on the dielectric interfaces.

Equations (11)–(13) and (15) are the principle contributions of this paper. Similar low-frequency approximations have been made to simplify the surface-wave field launched from a surface current on an open dielectric slab [6].

III. Verification

The following examples will be used for validation of the simplified formula presented above. Consider first the E_z-field in layer 1 due to a z-directed current I_z passing through layer 1. Using (11) and (15a), we get

$$E_z(x, y, z) = \frac{-k_o\eta_o\varepsilon_e^2}{4\varepsilon_{r1}^2(d_1 + d_2 + d_3)} H_o^{(2)}\left(\beta_o^{\mathrm{TM}}\rho\right) I_z d_1 \quad (16)$$

where ε_e is calculated from (8). As a second example, consider the E_z-field excited in layer 1 due to an x-directed current I_x of length L located at $\rho = 0$ on the surface of layer 1. Assuming that the observation point is $\rho = x$ and $y = 0$, (13) and (15a) result in

$$E_z(x, 0, z) = \frac{-k_o^2\eta_o\varepsilon_e^{3/2}(\varepsilon_{r1} - \varepsilon_e)d_1}{4\varepsilon_{r1}^2(d_1 + d_2 + d_3)} \frac{\partial H_o^{(2)}(p)}{\partial p} I_x L \quad (17)$$

where $p = \beta_o^{\mathrm{TM}} x$. Equations (16) and (17) are very simple equations. They can be evaluated using a calculator if the large argument approximation to the Hankel functions is made. Define the normalized field $\overline{E}_{zz}$ and $\overline{E}_{zx}$ to be the expressions that result when (16) and (17) are divided by $H_o^{(2)}$ and $\partial H_o^{(2)}/\partial p$, respectively. In addition, assume that $I_z d_1$ and $I_x L$ both equal 1 A · mm. Fig. 2 plots $\overline{E}_{zz}$ and $\overline{E}_{zx}$ versus frequency for a layer structure consistent with what can be found in a BGA [7]. Fig. 3 plots $\overline{E}_{zz}$ and $\overline{E}_{zx}$ for a layer structure that is representative of monolithic microwave integrated circuits (MMICs) in a multichip module if there is a uniform sealant layer.

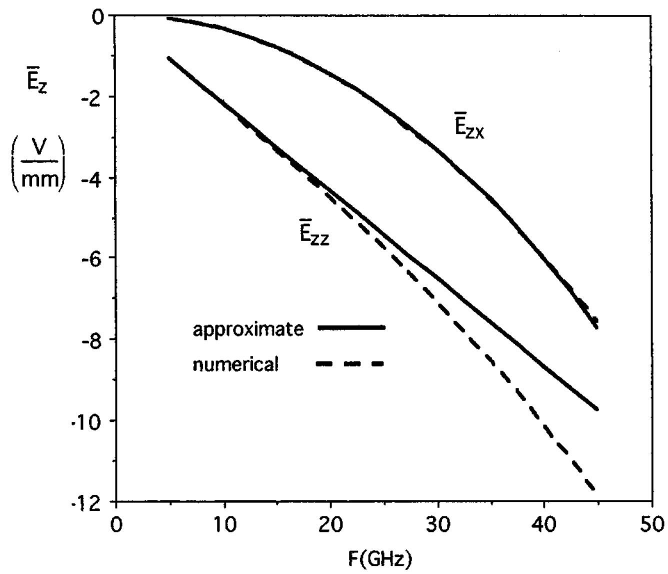

Fig. 2. Comparison of the frequency response of the normalized electric field calculated analytically (—) using the simplified equations and numerically (− − −). Results show fields generated by a surface current (E_{zx}) and by a via current (E_{zz}) when the layer structure is $d_1 = 0.4$ mm, $\varepsilon_{r1} = 4.4$, $d_2 = 0.7$ mm, $\varepsilon_{r2} = 1$, $d_3 = 0.375$ mm, $\varepsilon_{r3} = 9$.

To validate these equations, we also plot the more rigorous evaluation of $\overline{E}_{zz}$ at $z = d_1$ based on (4) and (14a). The residue of the full transcendental function Z_1 was evaluated numerically. The TM_o-mode propagation constant β_o^{TM} was evaluated by numerical solution of $Y_M(\beta) = 0$, where Y_M is given by (5). The reader is reminded that the only assumptions made to get E_z from (4) and (14a) is that the all TE and TM fields, except the TM_o mode are evanescent and have decayed to negligible levels at the observation point. $\overline{E}_{zx}$ at $z = d_1$ was evaluated in the same manner. These more rigorous evaluations of $\overline{E}_{zz}$ and

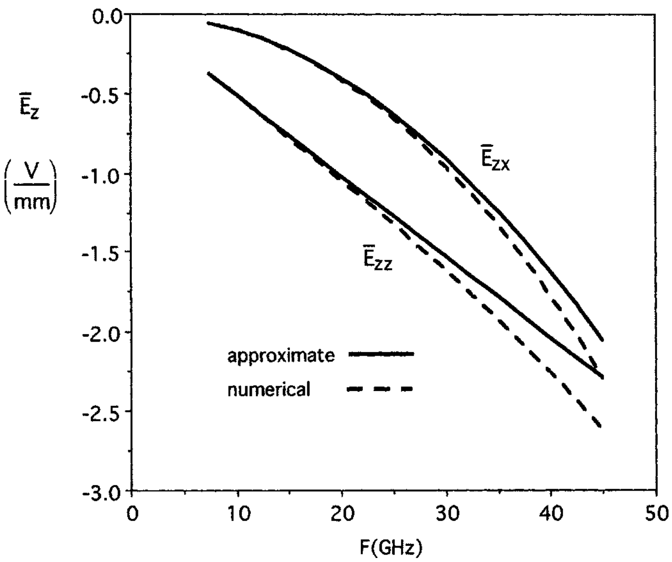

Fig. 3. Normalized electric fields generated when the layer structure is $d_1 = 0.1$ mm, $\varepsilon_{r1} = 12.9$, $d_2 = 0.1$ mm, $\varepsilon_{r2} = 3$, $d_3 = 0.3$ mm, $\varepsilon_{r3} = 1$.

$\overline{E}_{zx}$ are noted in Figs. 2 and 3 with a dashed line. For frequencies below 30 GHz, the agreement with the approximate calculations is better than 10%. The worst agreement is for the first layer set when the source is a z-directed current. Errors were under 20% at 45 GHz. In many applications, it is only necessary to know the coupling to within several decibels, and 20% error is quite acceptable. In addition, if the effective dielectric constant ε_e is determined from the numerically evaluated β_0^{TM} rather than from the approximate equation (8), then the 20% error at 45 GHz drops to under 4%.

IV. Disscussion

Simple expressions such as (11)–(13), and (15) are not only convenient to use, but they also give some insight into coupling between circuits in different parts of a structure. For purposes of calculating coupling within a multichip module, most radiating circuits can be approximated by a few electric dipoles [3]. Thus, the equations developed here will apply.

Using (16) and (17) as examples, we note that the field (and, thus, the coupling) from vias increases proportionally with frequency, but the field from surface currents increases like the square of frequency. By setting to one the magnitude of the ratio of (16) to (17) and recalling that, at large distances, the magnitude of the Hankel function and its derivative are equal, we find that the effective length of a surface current L_{xeq} needed to emit a field equal to the field emitted from a single via is

$$\frac{L_{xeq}}{d_1} = \frac{\lambda_o\sqrt{\varepsilon_e}}{2\pi d_1(\varepsilon_{r1} - \varepsilon_e)}. \tag{18}$$

Thus, for example, the layer structure described for Fig. 3 has an effective dielectric constant of 1.46. At 5 GHz, it would take a surface current as long as ten substrate thicknesses to radiate as effectively as a via through the substrate. The conclusion is that vias are an important source of coupling.

Equations (13) and (15b) show an interesting characteristic of coupling to surface currents. If the layer structure is chosen such that the effective dielectric constant of the TM_o parallel-plate mode is equal to the dielectric constant of substrate 1, then there will be no coupling to or from surface currents on the surface of substrate 1. As one would expect, (15c) shows the same effect for currents on the surface of substrate 3 if $\varepsilon_e = \varepsilon_{r3}$. For example, if the layer structure used for Fig. 2 were changed such the $\varepsilon_{r2} = 1$ and $\varepsilon_{r3} = 1.86$, then the effective dielectric constant will turn out to be 1.86 as well, and there will be no coupling to surface conductors on layer 3. There, however, will still be coupling between vias or between vias and surface currents on substrate 1. This type of design may be useful in some applications. The reader is cautioned that reactive field coupling will still occur, and that these conclusions are subject to the assumptions made in deriving (15).

Although the equations developed here assume a structure of infinite lateral extent, they also have ramifications for enclosed structures. If a rectangular package can be modeled as having either electric or magnetic sidewalls, then the field at a point inside is due to the field generated by the enclosed currents *plus* all the fields generated by images of the generating current in the enclosure side walls. Equations (11)–(13) and (15) would also apply for calculating the field from the images. Therefore, the degree of coupling within an enclosed package is also proportional to the factors present in the simplified equations.

V. Conclusions

A set of simple analytical equations has been derived for approximating the distant field generated by surface currents or vias in a three-layer parallel-plate structure. Such structures may be found in modern multilayer multichip microwave modules. The equations are valid at frequencies where only the lowest order parallel-plate mode is propagating. The effect of the layer structure on coupling between vias and surface currents is made evident by these equations.

Appendix A

The following quantities are often used in deriving spectral Green's functions in multilayer dielectrics. The derivation technique was originally developed by Itoh [2]

$$\tilde{Z}^e = Q_{\mathrm{TM}} \equiv \frac{1}{Y_M(\beta)} \equiv \frac{1}{Y_{\mathrm{LM}}^{(1)}(\beta) + Y_{\mathrm{RM}}^{(2)}(\beta)} \tag{A1}$$

$$Y_{\mathrm{LM}}^{(1)} = -jY_{\mathrm{TM}}^{(1)}\cot(k_{z1}d_1)$$
$$Y_{\mathrm{RM}}^{(3)} = -jY_{\mathrm{TM}}^{(3)}\cot(k_{z3}d_3) \tag{A2}$$

$$Y_{RM}^{(2)} = Y_{TM}^{(2)}\frac{Y_{RM}^{(3)} + jY_{TM}^{(2)}\tan(k_{z2}d_2)}{Y_{TM}^{(2)} + jY_{RM}^{(3)}\tan(k_{z2}d_2)} \tag{A3}$$

$$Y_{TM}^{(i)} = \frac{\varepsilon_{ri}k_o}{k_{zi}\eta_o} \quad k_{zi}^2 = \varepsilon_{ri}k_o^2 - \beta^2, \qquad \mathrm{Im}(k_{zi}) < 0.$$

Appendix B

The magnetic potential for a TM field in a three-dielectric-layer parallel-plate waveguide is shown in (A4) at the top of the following page.

$$A_z(x, y, z) = A_z(x, y, d_1) \begin{cases} \left[\cos(k_{z2}d_2) - \dfrac{\varepsilon_{r2}k_{z1}}{\varepsilon_{r1}k_{z2}} \tan(k_{z1}d_1)\sin(k_{z2}d_2)\right] \dfrac{\cos(k_{z3}[d_t - z])}{\cos(k_{z3}d_3)}, & d_1 + d_2 < z < d_t \\ \cos(k_{z2}[z - d_1]) - \dfrac{\varepsilon_{r2}k_{z1}}{\varepsilon_{r1}k_{z2}} \tan(k_{z1}d_1)\sin(k_{z2}[z - d_1]), & d_1 < z < d_1 + d_2 \\ \dfrac{\cos(k_{z1}z)}{\cos(k_{z1}d_1)}, & 0 < z < d_1 \end{cases} \tag{A4}$$

REFERENCES

[1] Y. L. Chow, J. J. Yang, D. G. Fang, and G. E. Howard, "A closed-form spatial Green's function for the thick microstrip substrate," in *IEEE Trans. Microwave Theory Tech.*, Mar. 1991, vol. 39, pp. 588–592.

[2] T. Itoh, "Spectral domain immitance approach for dispersion characteristics of generalized printed transmission lines," *IEEE Trans. Microwave Theory Tech.*, vol. MTT-28, pp. 33–736, July 1980.

[3] R. W. Jackson and Z. Wang, "Circuit model for coupling between MMIC's in multichip modules including resonance effects," *IEEE Trans. Microwave Theory Tech.*, vol. 46, pp. 959–964, July 1998.

[4] R. W. Jackson, "The use of sidewall images to compute package effects in MoM analysis of MMIC circuits," *IEEE Trans. Microwave Theory Tech.*, vol. 41, pp. 406–414, Mar. 1993.

[5] R. F. Harrington, *Time–Harmonic Electromagnetic Fields*. New York: McGraw-Hill, 1961.

[6] D. M. Pozar, "Rigorous closed-form expressions for the surface wave loss of printed antennas," *Electron. Lett.*, vol. 26, pp. 954–956, June 1990.

[7] R. Ito, R. W. Jackson, and T. Hongsmatip, "Modeling of electrical coupling between interconnections used in a multilayered BGA package," *IEEE Trans. Microwave Theory Tech.*, vol. 47, pp. 1819–1825, Sept. 1999.

Robert W. Jackson (M'82–SM'88) received the B.S., M.S., Ph.D. degrees from Northeastern University, Boston, MA, in 1975, 1979, and 1981, respectively.

From 1981 to 1982, he was an Assistant Professor in the Department of Electrical Engineering, Northeastern University. In 1982, he joined the University of Massachusetts at Amherst, where he is currently an Associate Professor. His primary research and teaching interests center on microwave and millimeter-wave electronics, especially ICs. In particular, he has contributed in the areas of numerical modeling of microstrip and coplanar-waveguide circuits, novel printed structures in coplanar waveguide, and the modeling of packages for microwave and millimeter-wave ICs. He has also developed computer-aided design (CAD) routines for ferrite phase-shifter design and consulted on topics connected with fiber optics for microwave applications.